Uncertainty, Climate Change and the Global Economy.*

David von Below † Torsten Persson ‡

February 28, 2008

Abstract

The paper illustrates how one may assess our comprehensive uncertainty about the various relations in the entire chain from human activity to climate change. Using a modified version of the RICE model of the global economy and climate, we perform Monte Carlo simulations, where full sets of parameters in the model's most important equations are drawn randomly from pre-specified distributions, and present results in the forms of fan charts and histograms. Our results suggest that under a Business-As-Usual scenario, the median increase of global mean temperature in 2105 relative to 1900 will be around 3.7 °C. The 99 percent confidence interval ranges from 2.5 °C to 5.7 °C. Uncertainty about socio-economic drivers of climate change lie behind a non-trivial part of this uncertainty about global warming.

*We are grateful for comments from Simon Dietz, Daniel Johansson, Karl-Göran Mäler, and Will Steffen. Financial support from the Swedish Research Council and Jan Wallander's and Tom Hedelius' Research Foundation is gratefully acknowledged.

†Institute for International Economic Studies, Stockholm University, SE-106 91 Stockholm. E-mail: david.vonbelow@iies.su.se.

‡Institute for International Economic Studies, Stockholm University, SE-106 91 Stockholm. E-mail: torsten.persson@iies.su.se.

1 Introduction

Uncertainty about future climate change is an unavoidable fact. It is commonplace to gauge this uncertainty by simulations with different climate models. This is the approach taken, e.g., by the International Panel on Climate Change (IPCC, 2001, 2007) to highlight our imprecise knowledge about the relation between specific atmospheric concentrations of greenhouse gases and global temperature. These model simulations typically rely on a small set of common and deterministic emission scenarios, so-called SRES-storylines (Nakićenović et al., 2000), which are not related to the processes underlying economic growth and energy use in an explicit and reproducible way. The approach is thus a partial one, focusing on specific biogeophysical relations in the complicated chain from human activity to climate change (and back). However, the socioeconomic relations behind regional and global economic growth, energy use and emissions are equally fraught with uncertainty as the biogeophysical relations.

A comprehensive assessment of the uncertainties about the important links in the chain from economic conditions to climate change is obviously a monumental task, and this paper is merely a first pass at the problem. Our approach is to simultaneously introduce uncertainty about a number of parameters that shape exogenous variables and endogenous relationships in the same simple, but comprehensive, model of the global climate and economy. We then perform Monte Carlo simulations, i.e., we make a large number of random draws of the full set of parameters and simulate the entire model for each such draw to derive probability distributions at different points in time for the variables of most interest.

Conceptually, our analysis is similar to that of Wigley and Raper (2001) who derive a probability distribution for future global mean temperature in a simple climate model, by introducing uncertainty through assigned probability density functions (p.d.f.) for the main drivers of temperature. However, their study stresses uncertainties in the biogeophysical and biogeochemical systems, while emissions are given by a (uniform) p.d.f. over alternative SRES scenarios, rather than alternative socioeconomic developments. A similar analysis is performed in the PAGE model (Hope, 2006) used in the Stern Review (Stern, 2007). Analogously, Murphy et al. (2004) derive a probability distribution for climate sensitivity (the effect on global mean temperature of doubled greenhouse gas concentration) from the Hadley Centre climate model, by drawing alternative values of the parameters that govern the model's important relations. While these studies focus on the physical and chemical systems, Nordhaus and Popp (1997) do consider uncertainty about socioeconomic drivers of climate change, but their purpose is different (to gauge the value of different types of scientific information).

Our analysis relies on a slightly modified version of RICE, an integrated model of climate and growth, developed and described by Nordhaus and

Boyer (2000). Section 2 gives a short description of that model and our modifications of it. Section 3 explains how we introduce uncertainty about model parameters. Section 4 presents results for variables of interest in two forms: fan charts, which illustrate how uncertainty develops over time, and histograms, which illustrate uncertainty at a point in time 100 years from now. Section 5 concludes.

2 The modified RICE model

We need a model that incorporates the global economy as well as the climate system and allows us to parametrically vary assumptions about important relations. For these reasons, we use an adapted version of the RICE–99 model, as formulated in Appendix D of Nordhaus and Boyer. (2000)[1] Next, we provide an overview of this model and our modifications. Equation numbers, variables, and parameters in brackets refer to a formal description of the model in the Appendix.

General description of RICE–99. The world is divided into eight regions (indexed by J) on the basis of geography as well as levels of economic development: United States (USA), OECD Europe (EUR), Other High Income countries (OHI), Russia and Eastern Europe (REE), Middle Income (MI), Lower Middle Income (LMI), China (CHI) and Lower Income (LI).[2] Neither trade nor investments flow between regions. Time (indexed by t) is measured in 10-year periods, starting in 1995. In each period, each region produces a homogeneous good with a neoclassical production technology based on capital and labor, but augmented by "energy services" reflecting the carbon content of energy inputs (see equation A.4). Regional damages from climate change are modelled as an output loss proportional to the value of GDP.

Economic growth in each region is driven by growth of population (A.5) and total factor productivity (TFP) (A.6). Higher economic growth implies more rapidly increasing regional demand for energy. How much this translates into use of exhaustible carbon resources depends on carbon-saving technological change (A.7), as well as regional energy prices. These prices have a regional component, reflecting regional taxes and distribution costs, and a global component, reflecting gradual exhaustion of the finite global supplies of oil, coal and natural gas (A.10-A.12). Naturally, higher prices curtail energy use.

Energy use in each region and time period creates industrial CO_2 emissions that, together with emissions from changes in land use and changes in

[1] This monograph gives a general description of the RICE model (chapter 2), and its appendix (pp. 179-187) includes all equations and parameter values of the baseline model.

[2] See Nordhaus and Boyer (2000) pp. 28–38 for definitions of regions.

the properties of the biosphere, end up in the global atmosphere (A.13). The model incorporates a simple carbon cycle, i.e., carbon flows between atmosphere, biosphere (cum shallow oceans), and deep oceans (A.14). Any CO_2 not absorbed in the ocean sinks adds to atmospheric concentration. Via increased radiation (A.15) more CO_2 raises global-mean surface temperature (A.16) in an amount depending on climate sensitivity.[3] Changes in climate create damages reflecting e.g., lower agricultural productivity, more frequent storms, or resettlements due to coastal flooding (A.17 and A.18). Damages, as a proportion of gross GDP, are region-specific quadratic functions of global temperatures in the period relative to 1900. Larger damages imply lower welfare. They also create a negative feedback effect, whereby lower output growth leads to less energy use ultimately reducing temperature.

Along an equilibrium time path of the model, consumers and producers in each region make decentralized utility and profit-maximizing decisions, adjusting savings and investments to the incomes, interest rates, technologies, and market prices they observe and rationally expect to prevail in the future. In particular, producers adjust their use of carbon-based energy to available technologies and regional energy prices. Regional and global welfare functions (A.1–A.3) are maximized in equilibrium.

RICE can be programmed and solved in two ways. The usual way is to maximize welfare, taking regional damages explicitly into account, so as to derive optimal uses of carbon-based energy, given their adverse effects via global temperature, and to calculate optimal carbon prices. Since our purpose is different, we do not take damages into account in the maximization. This way, we illustrate future paths in the absence of additional mitigation measures: Business As Usual (BAU) in the jargon of the climate-change literature.

Modifications We make a few adjustments to the RICE model, as follows.

Data for most variables entering the model are now available for the period 1996–2005 so we update initial values by one (ten-year) period and start off in 2005 rather than 1995. Atmospheric temperature for 2005 ($T(0)$ in A.16) comes from the UK Met Office, and atmospheric concentration of CO_2, ($M(0)$ in A.14) is obtained from the Carbon Dioxide Information Analysis Center[4] (CDIAC) and converted into a stock. The concentration of CO_2 in the upper oceans ($M_U(0)$ in A.14) is derived from the latter figure. Initial population figures for 2005 ($L_J(0)$ and $g_J^L(0)$ in A.5) come from the UN *World Population Prospects: The 2004 Revision Population*

[3]The climate-sensitivity parameter (κ) captures, in a very simple way, the complicated interactions in the geobiophyiscal earth system that produces a warmer climate as the atmospheric concentration of greenhouse gases goes up.

[4]The latest available figures for CO_2 concentration refer to 2004; linear extrapolation was used to get an estimate for the 2005 value.

Database. GDP figures for 2005 are collected from the World Bank's *World Development Indicators* database. These are used to calibrate initial levels of TFP, capital stocks, and energy services ($A_J(0)$, $K_J(0)$, and $ES_J(0)$ in A.6–A.9), assuming that investments and energy service inputs were chosen optimally in all regions between 1995 and 2005. Finally, we consider the TFP growth rate parameters in RICE–99 ($g_J^A(0)$ in A.6) too low and assign them higher values based on calculations from the Penn World Tables (Heston, Summers and Aten, 2002). Decline parameters for TFP growth (δ_J^A in A.6) are re-scaled accordingly. The precise numbers assigned to parameters and initial conditions are given in Tables 2 and 4 in the Appendix.

RICE assumes that the rate (all) consumers use to discount the utility of future consumption declines over time; we reset it to a constant. Specific assumptions about the discount rate are very important when using a climate model for the normative (prescriptive) purpose of finding optimal paths of mitigation (because abatement costs close in time are traded off against benefits of lower damages much further away in time).[5] For our specific positive (descriptive) purpose to illustrate uncertainty about future outcomes under BAU assumptions, the discount rate is much less important.

Finally, we try to incorporate scientific findings that the biosphere's ability to absorb CO_2 might change with climate.[6] At some level of CO_2 concentration in the atmosphere, the biosphere will likely switch from being a CO_2 sink to a CO_2 source. (Oceans too may absorb less CO_2 as climate changes, but these effects are smaller and less certain.) It is estimated that this terrestrial biosphere effect may contribute an additional 40–400 Gigatons of carbon (GtC) into the atmosphere by 2105, most models predicting a number between 100 and 200 GtC.

Ideally, the terrestrial biosphere effect should be added as an additional module to the climate part of the model. We have chosen a simpler solution: we just add an additional flow of emissions into the atmosphere in every period, calibrated to yield an average additional concentration in 2105 corresponding to 150 GtC. However, this value is highly uncertain, so we impose a probability distribution on it, as we do for many other model parameters.[7] The specification of such parameter uncertainties is the topic of the next section.

[5]The specific assumptions about the discount rate have indeed been one of the major points in the public discussion about the conclusions in the Stern Review (Stern (ed), 2006); see, e.g., Nordhaus (2006), Dasgupta (2007) and Weitzman (2007).

[6]This alteration of the model is based on personal communications with Will Steffen and on Friedlingstein et al. (2006).

[7]Specifically, these additional emissions are modelled with the following process:

$$TBE\,(t) = (\tau_1 + \tau_2\gamma)(t + \tau_3 t^2),$$

where scalars τ_1, τ_2 and τ_3 and random variable γ have been calibrated so that the terrestrial biosphere effect, on everage, adds 150 GtC in the atmosphere by 2105, with values falling between 40 and 400 GtC.

3 Introducing Uncertainty

We express the uncertainty about individual parameters and exogenous variables in the model as statistical distributions on the forms summarized in Tables 1, 2 and 4. Most distributions are assumed to be standard normals, but when they are deemed asymmetric we use beta distributions. The probability distribution for the climate sensitivity parameter is a special case derived from a truncated normal distribution, as discussed below.

Means for most parameters are close to the specific parameter values used in RICE, except that we raise the means of initial TFP growth rates to correspond more closely to the growth experience in the last ten years.

Using the p.d.f. of each one of the assumed distributions, we conduct a Monte Carlo simulation with 1001 independent random draws of the full set of parameters. For each of these draws, we carry out a full dynamic simulation for 400 years: an equilibrium time path of the model, as described above. These 1001 equilibrium paths generate different levels of GDP, emissions, temperatures, etc., which we use to describe the uncertainty about these outcomes.

Of course, each assumption regarding the distribution of an underlying parameter is a subjective assessment, made by ourselves or some collective of scientists. Most of the many relations that contribute to the climate problem are highly uncertain, however, and our objective is to illustrate a way to take this comprehensive uncertainty into account. We believe that the exercise meaningfully gauges the magnitude of uncertainty at different time horizons. Moreover, it helps illustrate the effects of favorable or unfavorable – from the viewpoint of climate change – circumstances, and which circumstances matter the most. Next, we provide details on the various sources of uncertainty.

Population Population growth is a major source of uncertainty about future output growth. In RICE, regional population trajectories are pinned down by two parameters: initial population growth rates, and the decline rates for population growth ($g_J^L(0)$, and δ_J^L in A.5). To calibrate these parameters, we rely on the UN *World Population Prospects: The 2004 Revision Population Database,* which contains forecasts for all countries in the world in five-year intervals up until 2050 in the form of three different scenarios: *low*, *median* and *high*. We aggregate these country scenarios up to RICE regions.

For five RICE regions (USA, REE, MI, LMI and LI), the UN forecasts and their implied uncertainty can be approximated very closely with model parameters. Mean values for initial population growth rates, $g_J^L(0)$, are set at the growth rate in the UN *median* scenario between 2000 and 2010, and mean values for decline in population growth, δ_J^L, are fitted using the 2005 and 2045 values for this scenario. We calibrate a p.d.f. for each regional

population by taking the *low* and *high* scenarios to correspond to ± 2 standard deviations, and use the value $\frac{1}{4}[g_J^L(0,high) - g_J^L(0,low)]$ as an estimate for the standard deviation. Similarly, the population growth decline parameters are fitted to the *low* and *high* scenarios, and $\frac{1}{4}[\delta_J^L(high) - \delta_J^L(low)]$ used as standard deviations.[8] Resulting means and standard deviations are reported in Table 4 in the Appendix.

In the remaining three regions (EUR, OHI, CHI), population levels are projected to first rise and then fall, which does not square with the parametrization in RICE. Mean population forecasts and the uncertainty around them are therefore entered manually up until 2045.[9] The mean and uncertainty about the post-2045 population growth rates are then parametrized by the same method as the one used from 2005 for the other five regions. Values for the post-2045 parameters are reported in Table 4 in the Appendix.

Figure 1 shows the median population trajectories for all regions and confidence bands around them in the form of fan charts.[10]

TFP Along with population growth, productivity growth is the most important determinant of future output levels. As mentioned above, we use higher initial TFP growth rates than RICE–99, namely the figures reported in Table 1, which we estimated based on the Penn World Tables data set. Decline parameters for TFP growth, δ_J^A, are scaled up by the same amount as the corresponding growth rates, $g_J^A(0)$.[11]

For five regions (US, EUR, OHI, CHI, LI), we judge that the distribution of initial TFP growth rates, $g_J^A(0)$, is skewed to the right. To achieve this, we use Beta distributions with parameters chosen to match our hypothesized

[8] An exception is *Russia and Eastern Europe*, where variability in δ_J^L needed to be reduced, or the population of REE would approach zero within the time frame of the program. Even though this region has a negative population growth rate, we do not expect its population to disappear entirely. The variability for the US also had to be reduced slightly, in order to avoid numerical problems with the most extreme draws.

[9] Specifically, quadratic functions of the form

$$L_J(t) = a_J + b_J t + c_J t^2$$

are fitted for each of the three regions to the *median* scenario values for 2005, 2025 and 2045. Here $t = 0$ corresponds to 2005, $t = 1$ to 2015 etc. Clearly, $a_J = L_J(0)$. To keep matters simple, b_J is kept constant and uncertainty introduced only on c_J. The average value of c_J is obtained directly from the *median* scenario, and variability for c_J is introduced such that the *low* and *high* scenarios represent ± 2 standard deviations around this mean for population in 2045. This way, the variabilities for the 2045 population levels (and hence also for later periods) are always kept on target.

[10] Throughout the paper, we choose to focus on the time period between now and 150 years ahead in the charts presented; however, the model simulations run through 40 time periods, i.e., 400 years.

[11] Before scaling, the TFP growth decline rate for OHI was raised to 1.5, the figure for USA and EUR. The low original value is likely due to assumptions about the structure of the Japanese economy; however such a difference between OHI and other OECD countries does not seem warranted on empirical grounds.

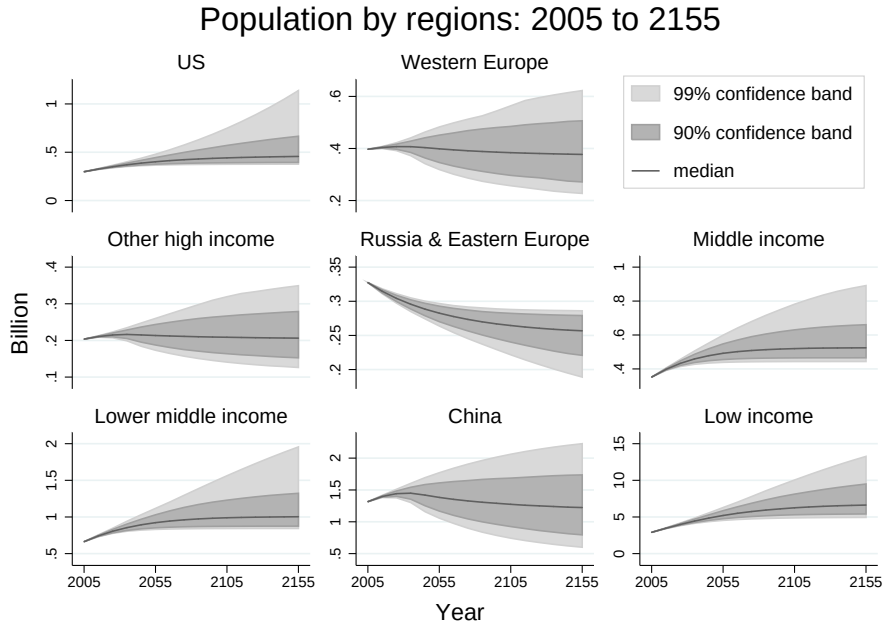

Figure 1: Forecasts for population levels, $L_J(t)$

mean and a variance of $(0.166)^2$. The figure 0.166 is the standard deviation of a Normal distribution normalized to have ± 3 standard deviations within a support of unity. The beta and normal distributions are then formulated in a consistent way. For all regions, the TFP growth decline rates, δ_J^A, are assigned normal distributions with a standard deviation of 20% of the mean value.

The regional TFP growth processes are modelled as independent of each other – i.e., in a particular model simulation, say, the US, may have rapid TFP growth while Europe's is slow. If technology spreads easily across

Region	Mean $g_J^A(0)$	St. dev. of $g_J^A(0)$	Type of distribution
USA	10.0	4.17	Beta, support $[5, 30]$
EUR	10.0	2.50	Beta, support $[5, 20]$
OHI	10.0	2.50	Beta, support $[5, 20]$
REE	15.0	3.33	Normal
MI	20.0	3.33	Normal
LMI	15.0	3.33	Normal
CHI	30.0	5.83	Beta, support $[20, 60]$
LI	25.0	6.67	Beta, support $[5, 40]$

Table 1: Uncertainties over TFP growth rates

countries and regions, one might think that technology shocks should be positively correlated. To address this concern, we have also run a version of the model where the TFP and energy efficiency processes have a (dominating) global component, alongside (less important) regional components. This specification made little difference to the results, but increased substantially the running time of the program. For this reason, we only report results for the simpler specification with independent technological growth processes across regions.

Figure 2 illustrates TFP forecasts in the form of fan charts (note the different scales on the y-axes).[12]

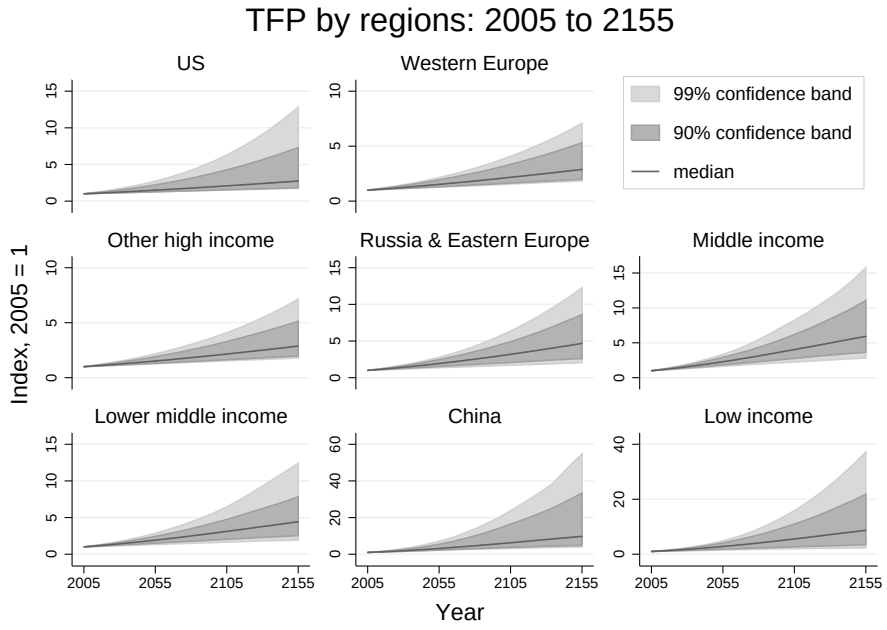

Figure 2: Forecasts for TFP levels, $A_J(t)$

Energy efficiency Energy efficiency in prodcution is modelled with parameter $Z_J(t)$, which is set at 1 in all regions in the initial period. Z then declines following a process similar to population and TFP growth, with an initial (negative) growth rate, $g_J^Z(0)$, and a decline parameter, δ_J^Z. A lower value of Z means higher energy efficiency: less CO_2 is emitted for the same amount of carbon energy used. Exploiting data on the ratio of CO_2 emissions to GDP, carbon intensity, from the World Bank *World Development*

[12]The Beta distributions of the underlying variables are clearly visible in the figure. Notice that also the regions where $g_J^A(0)$ is assumed to have a symmetric distribution end up with skewed distributions of TFP *levels*, $A_J(t)$, due the interaction between TFP *growth* parameters $g_J^A(0)$ and δ_J^A.

Indicators database, we estimate initial-period growth rates using data for the period 1997–2003. Specifically, we estimate mean yearly carbon intensity growth rates over this time period, and aggregate up to RICE regions and ten-year growth rates. In order to reduce the impact on carbon intensity of processes that are not proper improvements in energy efficiency (as defined in the model), we use an average between these estimates and the original RICE figures.

Looking at realized ratios of CO_2 emissions to GDP over time (i.e., from 1975 to 2003, the period where data exist), efficiency improvements indeed appear highly uncertain. Some countries seem to follow roughly a RICE type of process, in others CO_2/GDP ratios jump up and down almost randomly, while a few actually experience higher carbon intensity.[13] Of course, observed carbon intensities stem from various sources, including e.g., changes in product mix and development of alternative energy sources. In the end, we settled for a standard deviation of 30% of the mean value. This makes initial growth rates, $g_J^Z(0)$, relatively variable, but always contained in the range $[0, 2\mu]$, where μ denotes the mean value. Improvement decline parameters, δ_J^Z, are scaled up proportionally and given standard deviations of 20% of their means.

Figure 3 shows the forecasts for the energy efficiency parameter $Z_J(t)$.

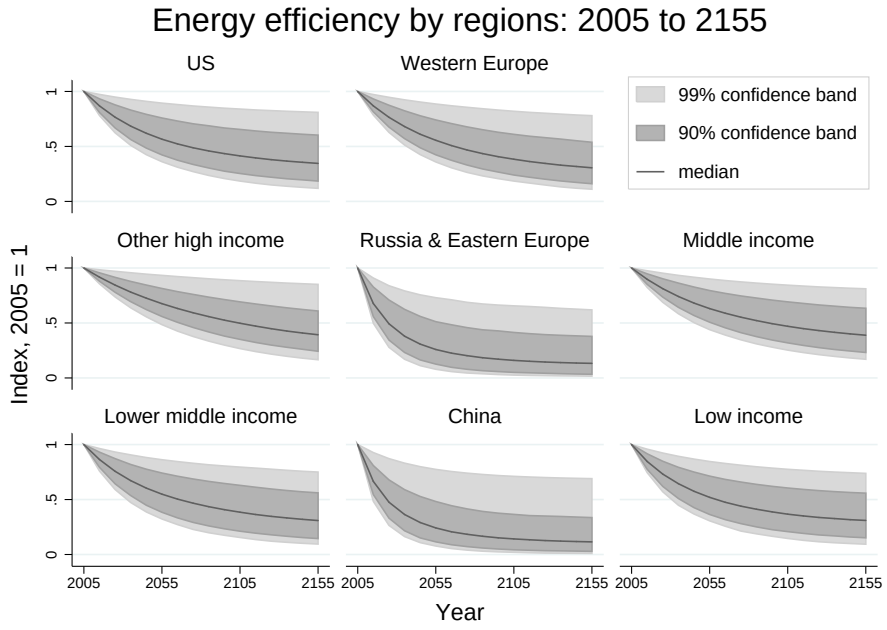

Figure 3: Forecasts for energy efficiency, $Z_J(t)$

[13] Brazil, Egypt, India, Iran, New Zealand, Portugal and Venezuela being a few examples.

Land use Emissions of CO_2 due to changes in land use arise mainly from deforestation: carbon of burnt biomass is released as carbon dioxide. In RICE, this process is modeled in similar fashion to other growth processes. Each region has an initial rate of emissions due to land use changes, and these rates then decline slowly at a rate set at 10% per decade.

We update initial emission rates and introduce uncertainty over them, based on figures in Chapter 7 of the WG1 contribution to the fourth IPCC Assessment Report (IPCC 2007). In particular, we use the disaggregated (Tropical Americas, Africa and Asia) AR4 estimates for the 1990s given in Table 7.2, interpreting the uncertainty ranges as ± 3 standard deviations.[14] The figures for the Lower Middle Income and especially Lower Income regions are revised upwards; for the other regions, changes are minor. Exact figures are reported in Table 4 in the Appendix.

Climate sensitivity The climate sensitivity parameter, κ, measures the rise in temperature following a doubling of atmospheric CO_2 concentrations. Many estimates of this parameter lie in the region around 3.0, but uncertainty about the true value is substantial and many climate models generate an asymmetric distribution. As explained by Roe and Baker (2007), a distribution with a pronounced right tail is a natural outcome of uncertainty about the various feedback processes whereby higher temperatures raise the level of radiative forcing. Examples of such feedbacks are changes in the formation of water vapor and clouds, or in the earth's albedo (ability to reflect solar radiation). In the RICE model framework, it is natural to portray the uncertainty about such fedbacks as uncertainty about climate sensitivity. We generate the latter following the same reduced-form approach as Roe and Baker. In their notation, we set (the average value and standard deviation of the feedback parameter) $f = 0.65$ and $\sigma = 0.10$, and in order to avoid extremely high (even infinite) values for κ, we truncate the distribution by cutting off 1% in the upper tail. Passing this truncated normal through the highly nonlinear transformation illustrated in Roe and Bakers's Figure 1, we obtain a p.d.f. similar in shape to the weighted p.d.f. reported in Figure 3 of Murphy et al. (2004).[15] The mean and median of this theoretical distribution are about 3.72 and 3.42 respectively. Figure 4 plots the frequency of draws, the realized p.d.f. for κ, used in our simulations.

[14] We take Lower Income countries to correspond to Tropical Africa and most of Tropical Asia, attributing the remaining fractions of the figure for Asia to Malaysia, which counts as Middle Income, and to China. The figure for Tropical Americas is divided equally between Middle Income (Brazil) and Lower Middle Income (most other Latin American countries).

[15] For Roe and Baker's ΔT_0, which they refer to as climate sensitivity in the absence of feedbacks, we use the value 1.2 °C.

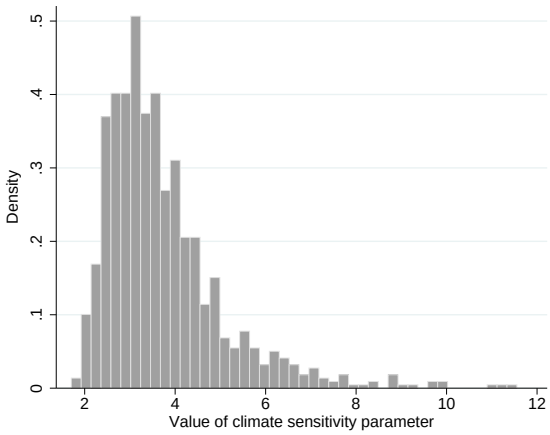

Figure 4: Distribution of draws on κ

Other uncertainties As mentioned above, we use a constant rate of time preference (ρ). The discount rate is assumed to have a normal distribution with standard deviation 0.33 around an average value of 3% (the initial rate in RICE). This way, random draws almost always fall within the range $[2, 4]$ with most outcomes within $[2.5, 3.5]$.

The regional coefficient on carbon-energy in the production function (β_J), the damage function parameters ($\theta_{1,J}$ and $\theta_{2,J}$), as well as the global carbon supply parameters (ξ_2, ξ_3 and $CMAX$) are assigned normal distributions with standard deviations 20% of their mean values.

4 Results

This section reports on selected results from our Monte Carlo simulations. To keep the presentation short, we focus here on the global variables of most interest.

World GDP Figure 5 shows future values of (the logarithm of) world GDP, measured in trillion USD (in 1990 prices).

The left panel illustrates the uncertainty with a fan chart, showing the median realization plus 90 and 99% confidence bands over the coming 150 years. The right panel shows a histogram of estimated world GDP 100 years ahead, which corresponds to an (unsmoothed) p.d.f. for that variable. Most of the uncertainty about future GDP levels stems from variability in TFP growth.[16] But variability in population growth and other exogenous

[16] A Regression of world GDP in 2105 on the realizations of all 16 TFP growth parameters within the same Monte Carlo draw gives an adjusted R-square of 0.718

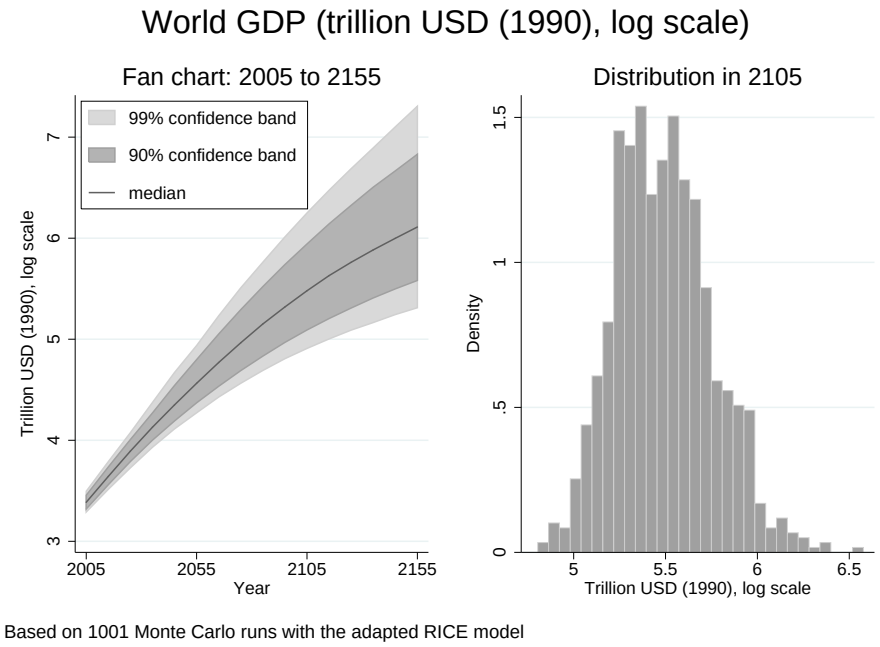

Figure 5: World GDP projections

parameters matters too, as does the fact that we report word GDP *net of* damages caused by rising global temperatures (as defined in A.17 and A.18).

As illustrated by the histogram and fan chart, the distribution is skewed to the right: i.e., we get relatively more extreme realizations of world GDP at the high end than at the low end. Note that there is actually a force pulling in the opposite direction: damages (to GDP) increasing more than proportionately with temperature, together with the right-skew in the p.d.f. of climate sensitivity, tend to produce a GDP distribution skewed to the left. However, this tendency is quantitatively completely swamped by the right-skew of the underlying TFP levels (recall the discussion in Section 3). Inspection of the simulation data reveals that the realizations in the right tail of the world GDP distribution are due to some combination of high growth rates in the US, China or low-income countries; the US because of its high initial GDP level, and the latter two because of their population size.

Industrial emissions Since production requires carbon energy as an input, higher GDP generally means higher industrial CO_2 emissions. However, substantial gains in energy efficiency allow incomes to grow without corresponding growth in emissions. Figure 6 illustrates future carbon emissions, measured in GtC. As the fan chart shows, uncertainty increases steadily over time, reflecting the increasing uncertainty about economic growth and

energy efficiency. Annual emissions in the median BAU realization reach their maximum more than a hundred years ahead, at almost three times their current level just below 10 GtC per year. Emissions then start to decline slowly, because carbon-saving technological change and the effect of higher carbon prices eventually outweigh the increased demand from higher world production. The upper part of the fan chart shows that in fifty of our 1001 simulations (i.e., 5%) industrial emissions peak at more than four times their current level.

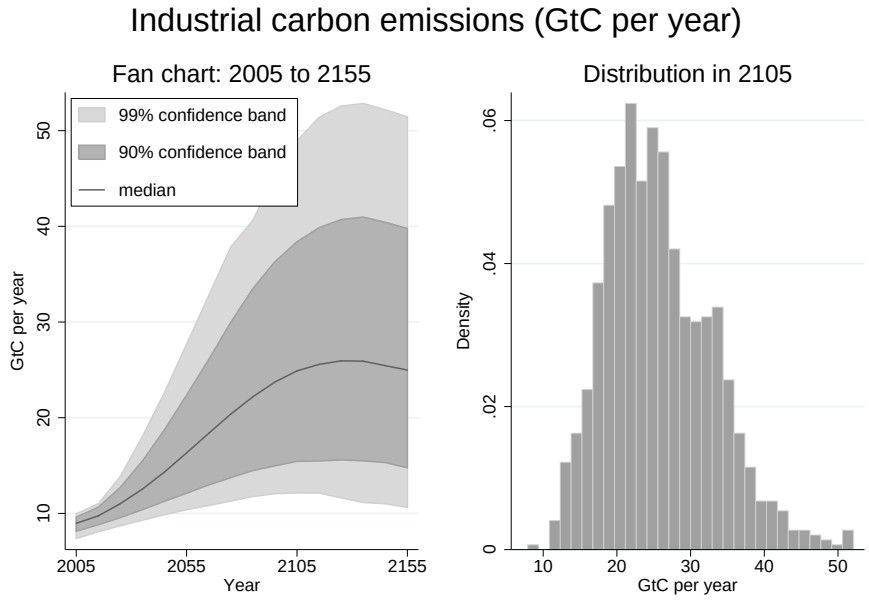

Figure 6: Projections for emissions of CO_2

The 2105 histogram clearly illustrates an upward skew in the emissions distribution. An important reason is the strong positive correlation between emissions and GDP levels (correlation about 0.53). The data shows that the extreme realizations in the right tail come about when either China or the group of low-income countries experience large increases in GDP growth but little improvement in energy efficiency. This is intuitive, given the population size of these regions, and their relatively poor initial energy efficiency.

Atmospheric concentration Because emissions, even in the low-growth BAU paths, are far larger than the earth's natural absorption capacity, they keep adding to the atmospheric concentration of CO_2 measured in parts per million (ppm). This is illustrated in Figure 7.

In the model, there is a close link between industrial CO_2 emissions and

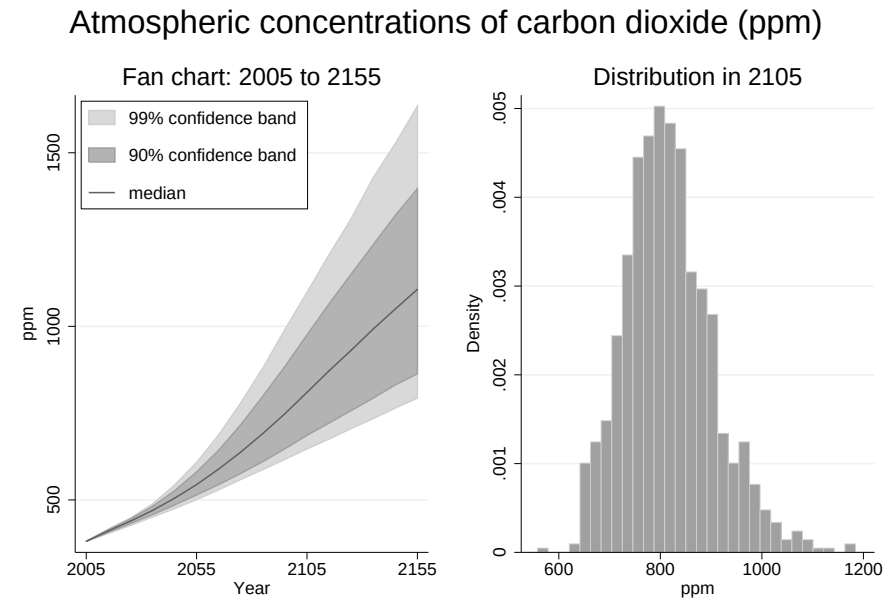

Figure 7: Projections for CO_2 concentrations

atmospheric concentration of carbon dioxide. The two are not perfectly correlated, however, given the uncertain terrestrial biosphere effect and uncertain regional changes in land use. Nevertheless, extreme values for CO_2 concentrations reflect the same causes as high industrial emissions. Since the carbon cycle is a slow process, the atmospheric concentrations adjust to emissions only with a long time lag, so we do not see a slowdown in the growth of CO_2 concentrations following the peak in emissions within the time frame of the fan chart.

Global warming Figure 8 shows future increases in global mean surface temperatures, relative to the year 1900, measured in Centigrades (°C). A century from now, the median realization of temperature is around 3 °C above today's temperature, which, in turn, is 0.71 °C above the 1900 level. A median temperature hike of 3 °C over a hundred years is broadly consistent with the median doubling of CO_2 concentration in Figure 7, and a median climate sensitivity of approximately 3.4 as discussed above.[17]

[17] Climate sensitivity refers to the long-run effect on temperature of a doubled CO_2 concentration, which is reached only with considerable time lag. This makes the actual rise in temperature between 2005 and 2105 fall short of 3.4 °C even though the concentration of CO_2 would double in that time. On the other hand, the model's temperature hike from 2005 to 2105 also incorporates lagged reactions to higher CO_2 concentrations before 2005. This adds an additional boost to 2105 temperature, above the value implied by the addition to CO_2 concentration between 2005 and 2105.

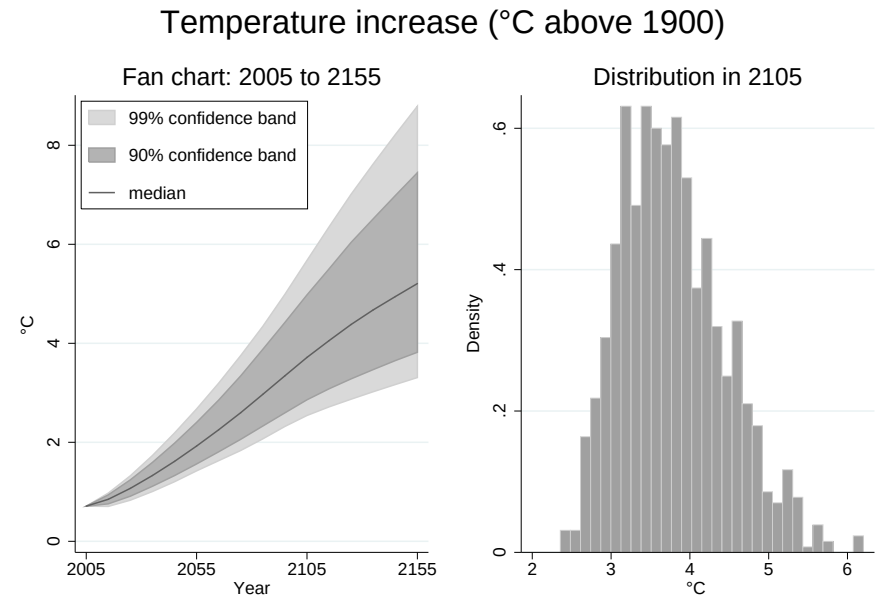

Figure 8: Temperature projections

What causes variability of global temperature in our simulations? The climate sensitivity parameter, κ, is the most important source of uncertainty.[18] This reflects the fact that climate sensitivity is the last link (in the RICE model) in the chain from human activity to global warming. In 2105, the 99% confidence interval for temperature is about 3 °C wide. This range of warming for the next century is of the same magnitude as the range reported elsewhere, but derived with very different methods (see e.g., IPCC 2001, 2007).

Notice that already the 5$^{\text{th}}$ percentile in Figure 8 lies clearly above 2 °C of warming. Indeed, the histogram in the right panel shows that all of the 1001 temperature realizations lie above the 2 °C line – the upper limit suggested in Article 2 of the UN framework Convention on Climate Change. Even the most optimistic realizations in the leftmost tail the for temperature should thus be a matter of grave concern.

Anyone who pays close attention to the optimistic tail, should seriously consider also the pessimistic tail of the distribution for climate change. As the histogram in Figure 8 shows, the highest temperature realizations by 2105 involve a rise around 6 °C. As is well-known the effects of such temperature changes are very hard to predict, but may include sea levels high enough to threaten major cities as London, Shanghai, or New York, and

[18] A regression of temperature increase in 2105 on values of draws on κ gives an adjusted R-square of 0.791.

substantial risks of large-scale shifts in the Earth system, such as collapses of the Gulf Stream or the West Antarctic ice sheet.

What realizations of the future lie behind the most severe instances of global warming? As already mentioned, climate sensitivity above its mean is a very important one. But other reasons are more squarely rooted in the human system. One is lower than expected improvements of energy efficiency in regions with high production and dirty technologies: chiefly the US and China. Another root is higher than expected economic growth in very populous regions, in particular the current low-income countries that host about half of the world population. To put it bluntly, futures in which today's unfortunate manage to permanently break out of poverty (without large improvements in energy-saving technologies) have substantially higher global warming. Ironically enough, resolution of one of today's most pressing global problems aggravates another one.

Figure 9 illustrates the interplay between different sources of climate change. The bottom right panel plots the temperature increase a hundred years from now against the randomly drawn value of the climate-sensitivity parameter (κ). A log curve approximates the relationship well, but the variability around this curve stems from variation in other parameters. We use the five highlighted observations, labeled 1 through 5 in all graphs, to discuss how GDP growth and energy efficiency matter for climate change. (Note that the temperature axis has the same scale in all four graphs.)

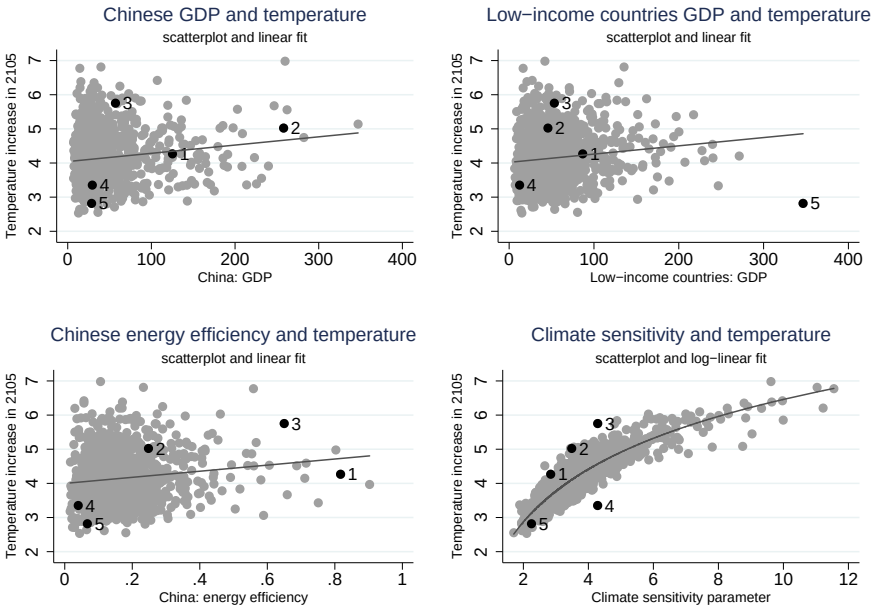

Figure 9: Illustration of sources of variability.

Observation 1 has the highest temperature increase, around 6.5 °C. Climate sensitivity is high, but temperature is still well above the fitted curve in the bottom right plot. This is due to very strong GDP growth in low-income countries (the GDP level in 2105 is at the 98^{th} percentile among 1001 simulations), and exceptionally low improvements in energy efficiency in China ($Z_{CHI}(2105)$ here takes its second-highest value out of the 1001 simulations; recall that less polluting outcomes correspond to lower values of "energy efficiency" as defined in the model). Observation 2, the most extreme outlier on the upside, also has temperature more than 6 °C above pre-industrial. This is due to high GDP growth in China, and also in the group of low-income countries. In addition, energy efficiency experiences little improvement in both regions. In observation 3, relatively high Chinese GDP growth interacts with one of the lowest improvements in Chinese energy efficiency (99^{th} percentile). US GDP (not shown) is also well above average. Observation 4 is the most extreme downside outlier, with about 1 °C lower temperature than what climate sensitivity predicts – and over 2 °C less than observation 3 (with rougly the same climate sensitivity). Explanations are to be found in low GDP growth in low-income countries, and in improvements in Chinese energy efficiency ($Z_{CHI}(2105)$ is at the 4^{th} percentile). Finally, observation 5 lies well below the fitted curve despite strong GDP growth in China. This is due to relatively high improvements in energy efficiency in the same region, and also to low GDP growth combined with high energy improvements in the US.

5 Conclusions

On the methodological side, we see the paper as illustrating a way forward in analyzing uncertainty about future climate change, which includes the most important determinants in the human system as well as the natural system. Our results suggest that uncertainties about relations in the economic system can play a major role. More research, with less stylized assumptions and more comprehensive climate-economy models, should follow.

On the substantive side, the simulations in this paper rely on BAU assumptions regarding energy taxes and other means of mitigating climate change. Our results show that, even under very favorable circumstances, global warming will be an increasing problem over the coming century.

Our simulations also show that damages[19] due to global warming are likely to strike very unevenly across the world's regions.

The fan charts in Figure 10 illustrate how the distributions of regional

[19] These damage estimates are derived using the RICE functional form and parameter values for damages, which are admittedly somewhat speculative. Even though absolute values of damages are highly uncertain, we believe that RICE captures the differences in vulnerability across regions.

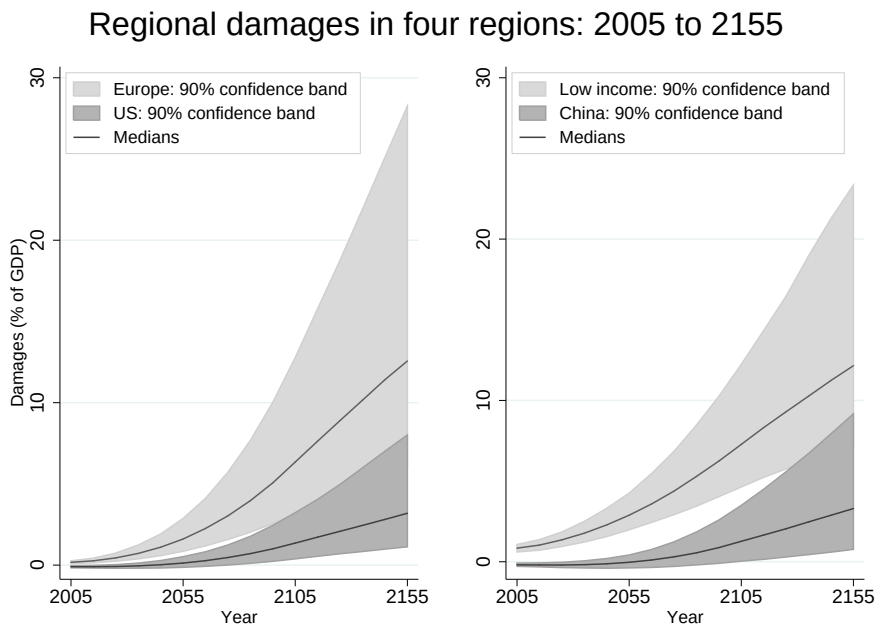

Figure 10: Regional damages in four regions

damages develop over time in four of the world's eight regions. A hundred years from now, the *upper* bound of the projected damages in low-damage regions USA and China more or less coincide with the *lower* bound on damages in high-damage regions Western Europe and Low-income countries. This suggests that conflicting political interests are likely to raise a higher hurdle than lack of scientific knowledge for agreements on global mitigation measures.

Appendix

This Appendix begins with a list of the full set of equations in the underlying RICE model. It also includes a list of all the model's variables and the distributions for the parameters we use in the Monte Carlo simulations.

RICE model equations

(A.1) $W_J = \sum_t U[c_J(t), L_J(t)]R(t)$

(A.2) $R(t) = \prod_t [1+\rho]^{-10t}$

(A.3) $U[c_J(t), L_J(t)] = L_J(t)\{log[c_J(t)]\}$

(A.4) $Q_J(t) = \Omega_J(t)\left\{A_J(t)K_J(t)^{\alpha}L_J(t)^{1-\beta_J-\alpha}ES_J(t)^{\beta_J} - c_J^E(t)ES_J(t)\right\}$

(A.5) $g_J^L(t) = g_J^L(0)\exp(-\delta_J^L t),\ g_J^L(0)$ given

$L_J(t) = L_J(0)\exp\left[\int_0^t g_J^L(t)\right],\ L_J(0)$ given

(A.6) $g_J^A(t) = g_J^A(0)\exp(-\delta_J^A t),\ g_J^A(0)$ given

$A_J(t) = A_J(0)\exp\left[\int_0^t g_J^A(t)\right],\ A_J(0)$ given

(A.7) $ES_J(t) = Z_J(t)E_J(t)$

$g_J^Z(t) = g_J^Z(0)\exp(-\delta_J^Z t),\ g_J^Z(0)$ given

$Z_J(t) = Z_J(0)\exp\left[\int_0^t g_J^Z(t)\right],\ Z_J(0) = 1$

(A.8) $Q_J(t) = C_J(t) + I_J(t)$

$c_J(t) = C_J(t)/L_J(t)$

(A.9) $K_J(t) = K_J(t-1)(1-\delta_K)^{10} + 10\times I_J(t-1),\ K_J(0)$ given

(A.10) $c_J^E(t) = q(t) + markup_J^E$

(A.11) $CumC(t) = CumC(t-1) + 10\times E(t)$

$E(t) = \sum_J E_J(t)$

(A.12) $q(t) = \xi_1 + \xi_2\left[CumC(t)/_{CMAX}\right]^{\xi_3}$

(A.13) $LU_J(t) = LU_J(0)(1-\delta_{LU})$

$ET(t) = \sum_J(E_J(t) + LU_J(t)) + TBE\,(t)$

$TBE\,(t) = (\tau_1 + \tau_2\gamma)(t + \tau_3 t^2)$

(A.14) $M(t) = 10\times ET(t-1) + \phi_{11}M(t-1) + \phi_{21}M_U(t-1),\ M(0)$ given

$M_U(t) = \phi_{12}M(t-1) + \phi_{22}M_U(t-1) + \phi_{32}M_L(t-1),\ M_U(0)$ given

$M_L(t) = \phi_{23}M_U(t-1) + \phi_{33}M_L(t-1),\ M_L(0)$ given

(A.15) $F(t) = \eta\left\{\ln[M(t)/M^{PI}]/\ln(2)\right\} + O(t)$

$O(t) = -0.1965 + 0.13465t \qquad t \le 10$

$\quad = 1.15 \qquad t > 10$

(A.16) $T(t) = T(t-1) + \sigma_1\left\{F(t) - \frac{\eta}{\kappa}T(t-1) - \sigma_2[T(t-1) - T_L(t-1)]\right\},\ T(0)$ given

$T_L(t) = T_L(t-1) + \sigma_3[T(t-1) - T_L(t-1)],\ T_L(0)$ given

(A.17) $D_J(t) = \theta_{1,J}T(t) + \theta_{2,J}T(t)^2$

(A.18) $\Omega_J(t) = 1/\left[1 + D_J(t)\right]$

List of variables and parameters

Exogenous variables and parameters	
$L_J(t)$	Population (millions)
$R(t)$	Social time preference discount factor
ρ	Social time preference discount rate
α	Elasticity of output w. r. t. capital
β_J	Elasticity of output w. r. t. energy services
$A_J(t)$	Total factor productivity (TFP)
$g_J^L(t)$	Population growth rate (percent per decade)
$g_J^L(0)$	Population growth rate in initial period
$\delta_J^L(t)$	Rate of decline of $g^L(t)$
$g_J^A(t)$	TFP growth rate (percent per decade)
$g_J^A(0)$	TFP growth rate in initial period
$\delta_J^A(t)$	Rate of decline of $g^A(t)$ (percent per decade)
$Z_J(t)$	Energy efficiency
$Z_J(0)$	Energy efficiency in initial period
$g_J^Z(t)$	Energy efficiency improvement rate (percent per decade)
$g_J^Z(0)$	Energy efficiency improvement rate in initial period
$\delta_J^A(t)$	Rate of decline of $g^Z(t)$ (percent per decade)
δ_K	Rate of depreciation of capital (percent per year)
$K_J(0)$	Initial capital stock
$markup_J^E$	Carbon services markup (1000 USD (1990) per ton carbon)
ξ_1	Marginal cost of carbon extraction in 1995
ξ_2, ξ_3	Parameters in cost-of-extraction function
$CMAX$	Point of diminishing returns in carbon extraction (GtC)
$LU_J(t)$	CO_2 emissions from land-use changes (GtC per year)
$LU_J(0)$	Emissions from land-use changes in initial period
δ_{LU}	Parameter in cost-of-extraction function
$TBE\,(t)$	Emissions due to the terrestrial biosphere effect
τ_1, τ_2, τ_3	Parameters in terrestrial biosphere process
γ	Random term in terrestrial biosphere process
η	Increase in forcing due to doubling of CO_2 concentrations
κ	Climate sensitivity parameter
σ_1	Speed of adjustment for atmospheric temperature
σ_2	Coefficient of heat loss from atmosphere to deep oceans
σ_3	Coefficient of heat gain from atmosphere to deep oceans
$\theta_{1,J}$	Coefficient on linear component in damage function
$\theta_{2,J}$	Coefficient on quadratic component in damage function
Carbon cycle transition coefficients (percent per decade):	
ϕ_{11}	Atmospere to atmosphere
ϕ_{12}	Atmosphere to upper box
ϕ_{21}	Upper box to atmosphere
ϕ_{22}	Upper box to upper box
ϕ_{23}	Upper box to lower box
ϕ_{32}	Lower box to upper box
ϕ_{33}	Lower box to lower box

Initial conditions (temperatures relative to 1900):	
$M(0)$	Initial stock of carbon in the atmosphere (GtC)
$M_U(0)$	Initial stock of carbon in the upper ocean (GtC)
$M_L(0)$	Initial stock of carbon in lower ocean (GtC)
M^{PI}	Preindustrial stock of carbon in atmosphere (GtC)
$T(0)$	Initial atmospheric temperature (°C)
$T_L(0)$	Initial ocean temperature (°C)
Endogenous variables:	
$W_J(t)$	(Global) Welfare
$U_J(t)$	(Regional) Utility
$c_J(t)$	Per-capita consumption
$Q_J(t)$	Output (trillion 1990 USD per year)
$K_J(t)$	Capital stock (trillion 1990 USD)
$ES_J(t)$	Energy services from fossil fuels (GtC per year)
$E_J(t)$	Industrial CO_2 emissions (GtC per year)
$C_J(t)$	Consumption (trillion 1990 USD per year)
$I_J(t)$	Investment (trillion 1990 USD per year)
$CumC(t)$	Cumulative industrial carbon emissions (GtC)
$ET(t)$	Total global carbon emissions (GtC per year)
$M(t)$	Atmospheric CO_2 concentration (GtC)
$M_U(t)$	CO_2 stock in the upper oceans and biosphere (GtC)
$M_L(t)$	CO_2 stock in the upper oceans (GtC)
$F(t)$	Increase in forcing relative to preindustrial (W/m^2)
$T(t)$	Atmospheric temperature increase since 1900 (°C)
$T_L(t)$	Temperature increase in lower oceans since 1900 (°C)
$D_J(t)$	Climate change damages (proportion of output)

Table 2: Global parameters: updated values and imposed uncertainty

name	original value	updated value	standard deviation*
ρ	3.00	—	0.33
ξ_2	700	—	140
ξ_3	4.00	—	0.8
$CMAX$	6000	—	1200
γ	—	**	**
κ	2.9078	***	***
$M(0)$	735	811	—
$M_U(0)$	781	820	—
$M_L(0)$	19230	—	—
M^{PI}	596.4	—	—
$T(0)$	0.43	0.71	—
$T_L(0)$	0.06	—	—

* *Probability distributions are standard normals unless indicated.*

** *Distributed as Beta(1.5, 3.5), which gives a mean value of 0.3.*

*** *See discussion in Section 3 and Figure 4 above.*

Table 3: Unchanged and deterministic global parameters

name	value	name	value	name	value
α	0.30	τ_3	0.10	ϕ_{12}	33.384
δ_K	10	η	4.10	ϕ_{21}	27.607
ξ_1	113	σ_1	0.226	ϕ_{22}	60.897
δ_{LU}	10	σ_2	0.440	ϕ_{23}	11.496
τ_1	0.07	σ_3	0.02	ϕ_{32}	0.422
τ_2	0.64	ϕ_{11}	66.616	ϕ_{33}	99.578

Table 4: Regional parameters: updated values and imposed uncertainty

name	USA	EUR	OHI	REE	MI	LMI	CHI	LI
$LU_J(0)$	0	0	0	0	.40	.35	.05	1.00
	(0)	(0)	(0)	(0)	(.058)	(.05)	(.0083)	(.15)
$L_J(0)$	298.2	397.1	203.6	327.4	351.9	663.1	1315.8	2906.5
	(–)	(–)	(–)	(–)	(–)	(–)	(–)	(–)
$g_J^L(0)$	9.89	-1.26*	-0.82*	-4.27	14.53	13.12	-2.87*	19.60
	(0.45)	(2.34)	(2.27)	(0.46)	(0.54)	(0.56)	(2.77)	(0.52)
δ_J^L	22.23	15.00	15.00	15.66	36.52	31.48	15.00	23.00
	(7.50)	(5.00)	(5.00)	(5.00)	(9.23)	(9.19)	(5.00)	(5.06)
$g_J^A(0)$	10**	10**	10**	15	20	15	30**	25**
	(4.17)	(2.50)	(2.50)	(3.33)	(3.33)	(3.33)	(5.83)	(6.67)
δ_J^A	3.9	3.8	3.7	5.5	7.5	6.1	10	8.3
	(– – – – – – – – – – – – *20% of the mean value* – – – – – – – – – – – –)							
$g_J^Z(0)$	-15.0	-14.6	-8.8	-43.4	-11.5	-15.8	-45.1	-18.0
	(– – – – – – – – – – – – *30% of the mean value* – – – – – – – – – – – –)							
δ_J^Z	11.59	9.14	4.94	20.36	8.86	10.24	19.76	13.52
	(– – – – – – – – – – – – *20% of the mean value* – – – – – – – – – – – –)							
β_J	.091	.057	.059	.08	.087	.053	.096	.074
	(– – – – – – – – – – – – *20% of the mean value* – – – – – – – – – – – –)							
$markup_J^E$	300.0	400.0	350.0	-38.12	250.0	-2.63	-41.09	18.78
	(–)	(–)	(–)	(–)	(–)	(–)	(–)	(–)
$\theta_{J,1}$	-.0026	-.001	-.007	-.0076	-.0039	-.0022	-.0041	.01
	(– – – – – – – – – – – – *20% of the mean value* – – – – – – – – – – – –)							
$\theta_{J,2}$	.0017	.0049	.003	.0025	.0013	.0026	.002	.0027
	(– – – – – – – – – – – – *20% of the mean value* – – – – – – – – – – – –)							

Mean values are reported, standard deviations (where applicable) in parentheses. The values of $L_J(0), g_J^L(0), \delta_J^L, g_J^A(0)$ and δ_J^A have been updated; original values are not reported. All parameters are normally distributed, except where indicated. All rates are percentages per decade.

* *"Initial" growth rates here refers to 2045, see Section 3 for details.*

** *These parameters have Beta distributions. All are right-skewed.*

References

[1] Sir P. Dasgupta, "Comments on the Stern Review's Economics of Climate Change", *National Institute Economic Review* 199, 2007.

[2] Friedlingstein. P., Cox, P., Betts, R., Bopp, L., von Bloh, W., Brovkin, V, Doney, S., Eby, M., Fung, I., Govindasamy, B., John, J., Jones, C., Joos, F., Kato, T., Kawamiya, M., Knorr, W., Lindsay, K., Matthews, H. D., Raddatz, T., Rayner, P., Reick, C., Roeckner, E., Schnitzler, K.-G., Schnur, R., Strassmann, K., Thompson, S., Weaver, A. J., Yoshikawa, C., and Zeng, N., "Climate-Carbon Cycle Feedback Analysis, Results from the C4MIP Model Intercomparison", *Journal of Climate* 19(14):3337–3353, 2006.

[3] Heston, A., Summers, R., and Aten, B., *Penn World Table Version 6.1*, Center for International Comparisons at the University of Pennsylvania (CICUP), October 2002.

[4] Hope, C., "The Marginal Impact of CO_2 from PAGE2002: An Integrated Assessment Model Incorporating the IPCC's Five Reasons for Concern", *Integrated Assessment Journal* 6, 19-56, 2006.

[5] IPCC, *Climate Change 2001: The Third Assessment Report of the Intergovernmental Panel on Climate Change*, Cambridge Univ. Press, Cambridge, 2001

[6] IPCC, *Climate Change 2007: The Fourth Assessment Report of the Intergovernmental Panel on Climate Change*, Cambridge Univ. Press, Cambridge, 2007

[7] Murphy, J., Sexton, D., Barett, D., Jones, G., Webb, M., Collins, M., and Stainforth, D., "Quantification of Modelling Uncertainties in a Large Ensemble of Climate Change Simulations", *Nature* 430:768–772, 2004.

[8] Nakićenović, N. et al., *Emission Scenarios. A Special Report of Working Group III of the Intergovernmen-tal Panel on Climate Change,* Cambridge University Press, Cambridge, U. K., 2000

[9] Nordhaus, W. D., "The Stern Review on the Economics of Climate Change", Mimeographed, Yale University, November 2006.

[10] Nordhaus, W. D. and Boyer, J., *Warming the World: Economic Models of Global Warming*, MIT Press, Cambridge, MA, 2000.

[11] Nordhaus, W. and Popp, D.,"What is the Value of Scientific Knowledge," *The Energy Journal* 18, 1-45, 1997.

[12] Roe, G. H. and Baker, M.B., "Why Is Climate Sensitivity So Unpredictable", *Science* 318, 629–632, 2007.

[13] Sir N. Stern (ed), *The Stern Review on the Economics of Climate Change*, Cambridge Univ. Press, Cambridge, 2006.

[14] Weitzman, M., in press, "The Stern Review of the Economics of Climate Change", *Journal of Economic Literature*.

[15] Wigley, T. M. L. and Raper, S. C. B., "Interpretation of High Projections for Global-Mean Warming", *Science* 293, 451–454, 2001.